Response evaluation and follow-up by imaging in brain tumours

Chapter 26 in

Imaging and interventional Radiology for Radiation Oncology

Renske Gahrmann

Javier Arbizu

Anne Laprie

Maribel Morales

Marion Smits

ACCEPTED

ABSTRACT

Brain tumours, either primary or secondary, are frequent. Primary brain tumours include mainly glioma, lymphoma and meningioma. Secondary tumours, i.e. brain metastasis, are a frequent event during the disease course of patients with cancer. The evaluation of response to treatment is often difficult with structural imaging due to the interference of treatment effects. In this chapter, the role of advanced imaging for the differential diagnosis between pseudoprogression, radiation necrosis and tumour recurrence is described with perfusion and diffusion MR imaging, MR spectroscopy, and PET imaging with amino acid analogues, fluorodeoxiglucose and other tracers. Furthermore, the commonly used response criteria for various brain tumours are described. For glioma, these are those set out by the Response Assessment in Neuro-Oncology (RANO) group. For brain metastases the RANO-brain metastasis (RANO-BM) and RECIST criteria are commonly used. While conventional T1w post-contrast imaging is the mainstay imaging modality for basic response assessment, multimodal imaging is commonly necessary to evaluate the response to treatment of primary and secondary brain tumours.

INTRODUCTION

Brain tumours can be either primary (gliomas, lymphomas, meningiomas) or secondary (metastases). They carry a substantial burden of severe symptoms and complications. Their treatment often includes radiotherapy. The evaluation of tumour response can be challenging particularly in gliomas with the issue of pseudoprogression. For all tumours, another challenge is to differentiate radiation necrosis from tumoural residue or recurrence. The use of advanced imaging modalities is commonly useful in these situations.

Imaging methods

Structural imaging

Treatment response assessment of brain tumours is generally performed using structural magnetic resonance (MR) images, such as T2-weighted (T2w), T2w Fluid Attenuation Inversion Recovery (FLAIR), and pre- and post-contrast T1-weighted (T1w) imaging. Most tumours show enhancement on post-contrast T1w images and 2D measurements on this sequence remain the basis of treatment assessment.

Additional information on tumour pathophysiology can be obtained with advanced MR imaging techniques and nuclear medicine imaging.

Advanced MR imaging

Diffusion weighted imaging (DWI) and diffusion tensor imaging (DTI) can be considered as both structural and functional techniques. The amount of diffusion (or random motion) of water molecules is measured with DWI. In DTI, diffusion is measured in multiple directions (minimum of 6) to calculate the tensor or general direction of diffusion. Diffusion can be limited due to structures within the voxel. In tumour, high cellular density restricts diffusion, which is reflected in the DWI-derived Apparent Diffusion Coefficient (ADC)[1]. DTI-derived measures include fractional anisotropy (FA), which provides information on the degree of directional diffusion along the three main axes, and mean diffusivity (MD), which is similar to ADC[2]. It is important to note that ADC is not only influenced by extracellular space tortuosity, but also by membrane damage and perfusion[3].

Most commonly used for *perfusion imaging* is T2*-weighted dynamic susceptibility-weighted contrast-enhanced (DSC) imaging. When the blood-brain-barrier is breached, contrast-agent leaks from the vessels into the surrounding tissue, increasing T1w-signal intensity and decreasing the T2*-signal. This effect must be counteracted (either in advance or during post-processing) when maps of relative cerebral blood volume (rCBV) are calculated, but can also be used to calculate other parameters, such as the peak height (PH) and percentage signal intensity recovery (rPSR)[4]. Other

perfusion techniques include dynamic contrast enhanced (DCE) imaging and arterial spin labelling (ASL). DCE-derived measures include cerebral blood flow (CBF), capillary permeability (K^{trans}), and extravascular extracellular volume fraction (V_e)[5]. Where for both DSC- and DCE-imaging intravascular injection of contrast-agent is required, the blood itself forms the contrast in arterial spin labelling (ASL). ASL-derived CBF has been shown to correlate well with DSC-derived rCBV measures[6].

In *MR spectroscopy* different resonance frequencies of specific molecules and metabolites can be measured within different tissues, most commonly using protons (^{1}H-MRS). In brain tumours, N-acetyl aspartate (NAA), Choline (Cho), myo-Inositol (mI), lactate/lipid Lac), and Creatine (Cr) are commonly assessed, although many more may be measured[7].

Chemical Exchange Saturation Transfer (CEST) imaging is a more recent technique, which can be used to measure amides (-NH), amines (-NH_2), and hydroxyl (-OH) groups among others, but is still very much in the research arena[8].

Nuclear medicine imaging

Nuclear medicine techniques such as single photon tomography (SPECT) and positron emission tomography (PET) are being used worldwide for the characterisation, therapy planning and recurrence assessment of brain tumours. SPECT using cellular viability radiotracers like as 99mTechnetium- sestamibi (99mTc-MIBI) and 201Thallium were initially employed in clinical practice due to its high availability[9,10]. However, in recent years PET has been gradually introduced into the clinical practice instead of SPECT for the evaluation of brain tumours as a complementary and supplementary tool of standard MR imaging sequences. It is important to note that fusion images between structural (computed tomography (CT) and/or MR imaging) and PET or SPECT images are highly recommended to achieve better accuracy. Multimodality systems are now available that combine SPECT and PET scanners and structural imaging devices like CT (SPECT-CT and PET-CT) and more recently MR imaging (PET-MR imaging). Visual analysis of images is the most common method for scan evaluation in clinical practice. The study is classified as positive when the activity observed in the lesion exceeds the reference region (usually normal cortex). However, semiquantitative analysis of PET studies can also be performed using the standard uptake value (SUV), commonly calculated for quantifying systemic tumours. This parameter however has a limited role in the clinical interpretation of images in neuro-oncology. Instead, tumour or lesion to brain reference region ratios using mean or maximum SUV (TBR) are used to provide a measure of PET radiotracers uptake in brain tumours.

One of the hallmarks of PET is the variety of parameters that can be observed and measured in brain tumours by means of specific radiotracers. Some of the most commonly used in clinical practice are reviewed in this section.

Glucose metabolism

Brain 2-deoxy-2-[18F]-2-fluoro-2-deoxy-D-glucose (FDG) uptake is usually acquired 45 to 60 minutes after the injection of 185 MBq of FDG. Patients must be fasting for 4 hours prior to injection, and it is recommended to obtain a measurement of blood glucose prior to the exam: high blood glucose levels at the time of injection decreases uptake in tumour and healthy tissue, although it may not affect lesion detection detectability. In case sedation is required, this can be carried out 45-60 minutes after injection, just prior to the time of the acquisition[11].

FDG accumulates in the majority of tumours due to elevated glucose metabolism in response to increased energy demand. This technique has been applied to brain tumour imaging for many years. The relationship of FDG uptake to tumour glioma grade and prognosis has been reported in several studies[12]. However, FDG is in some way limited in neuro-oncology due to the high rate of glucose metabolism in normal brain parenchyma resulting in diminished signal-to-noise ratio for brain tumours. Another problem with FDG is the high uptake of this tracer in inflammatory cells, which can occur in a variety of disease processes and can be independent of tumour growth or response[13]. Consequently, as newer PET tracers have become available, the use of FDG for imaging in neuro-oncology has declined.

Amino acid transport

System L amino acid transport PET radiotracers ([11C-methyl]-methionine (-MET), O-(2-[18F]-fluoroethyl)-L-tyrosine (FET) and 3,4-dihydroxy-6-[18F]-fluoro-L-phenyl-alanine (FDOPA) are currently used in neuro-oncology. MET has been used since 1983[14], but is limited to centres with an on site cyclotron because it is labelled with ^{11}Carbon, a radioisotope with a very short half-life (20 minutes). FET and FDOPA are labelled with ^{18}Fluorine, a radioisotope with a longer half-life, which allows radio-tracer transportation from the manufacturing laboratory to the PET centre[12].

The uptake of radiolabelled amino acids observed in normal brain tissue as well as in brain lesions including tumours of many types is predominantly conditioned by the transmembrane active transport, which is responsible for the biological activity in tissues, including cell proliferation. The uptake by cerebral tumour tissue appears to be caused almost entirely by increased transport via the specific amino acid transport system L for large neutral amino acids[12]. The uptake is also influenced by passive diffusion in regions with blood-brain-barrier disruption, and by stagnation in regional vascular beds that depends on blood volume due to a large vascular bed[15]. In contrast to tumour, the uptake of radiolabelled amino acids in normal brain is very low resulting in a high contrast between tumour and normal brain tissue.

After a recommended period of 4 hours of fasting, 200 MBq of FET, 370-555 MBq of MET, or 185 MBq of FDOPA are injected and a static PET acquisition is performed

20 minutes later. In addition to static images, dynamic FET PET data can be acquired, which allows the characterisation of the temporal pattern of FET uptake by deriving a time-activity curve (TAC) in brain tumours[16,17]. It remains to be shown, however, whether dynamic MET and FDOPA can contribute significantly to the characterisation of brain tumours. The more widespread use of amino acid PET for the management of patients with brain tumours has been strongly recommended by the Response Assessment in Neuro-oncology (RANO) group[13,18].

Somatostatine receptors

The most common somatostatin receptor (SSTR) radioligands for PET imaging are 68Ga-DOTA-Tyr3-octreotide (68Ga-DOTATOC), 68Ga-DOTA-D-Phe1-Tyr3-octreotate (68Ga-DOTATATE) or 68Ga-DOTA-l-Nal3-octreotide (68Ga-DOTANOC). These radiotracers, frequently used for imaging of neuroendocrine tumours, have been introduced in neuro-oncology due the overexpression of SSTR subtype 2 in almost all meningiomas[19]. 68Ga has a physical half-life of 68 minutes and can be produced with a 68Ge/68Ga generator system, which enables in-house production without the need for an on-site cyclotron. PET ligands to SSTR provide high sensitivity with excellent target-to-background contrast due to low uptake in bone and healthy brain tissue[20].

There are no comparative studies of 68Ga-DOTATOC, 68Ga-DOTATATE and 68Ga-DOTANOC, but the uptake of all these tracers is relatively high compared to normal brain; thus, possible differences between these tracers are not really relevant. Procedure guidelines for PET imaging with 68Ga-DOTA-conjugated peptides have been published recently[21].

Other radiotracers

Several other radiotracers are used to image brain tumours. The *thymidine nucleoside analogue 3'-deoxy-3'-18F-fluorothymidine* (*FLT*) is a substrate for thymidine kinase-1 and reflects cell proliferation. Although previous studies suggest that FLT is a promising tool for glioma detection and grading[22] and is able to predict improved survival after bevacizumab therapy[22,23], the uptake of this tracer is dependent on disruption of the blood-brain barrier, thereby limiting its clinical value.

Hypoxia in brain tumours has been demonstrated with use of the PET tracer *18F-Fluoromisonidazole* (*FMISO*)[24]. FMISO enters tumour cells by passive diffusion and becomes trapped in cells with reduced tissue oxygen partial pressure by nitroreductase enzymes. This tracer thus allows the identification of hypoxic tumour areas, which are thought to be more resistant to irradiation[25], as well as a trigger for neoangiogenesis. Thus far, FMISO has predominantly been used in a preclinical setting.

Another interesting PET target is the *translocator protein* (*TSPO*), a mitochondrial membrane protein that has been used as biomarker for neuroinflammation. TSPO is

highly expressed in activated microglia, macrophages and neoplastic cells. Imaging with the TSPO ligand 11C-(R)PK11195 demonstrates increased binding in high-grade glioma compared to low-grade glioma and normal brain parenchyma[26]. More recently, the TSPO ligand 18F-DPA-714 labelled with 18F has been evaluated in glioma animal models[27].

Choline is a marker of phospholipid synthesis involved in the synthesis of cell membrane components. The *radiolabelled choline* (either ^{11}Carbon and more recently ^{18}Fluorine) is trapped by glioblastoma with a very high contrast to normal brain, whereas its role in lower grade gliomas is limited[28]. When compared with FDG, radiolabelled choline appears to be superior in terms of diagnostic performance in glioma and metastasis[29].

TREATMENT RESPONSE

Glioma

Background

Newly diagnosed anaplastic glioma and glioblastoma (GBM) are the most frequent primary brain tumours in adults. They are treated with the Stupp protocol, consisting of surgery, whole-brain radiotherapy (WBRT) and temozolomide (TMZ), followed by adjuvant TMZ. In diffuse low-grade gliomas the presence of certain negative prognostic factors can be considered a reason for adjuvant radiotherapy[30]. The effects of radiotherapy combined with TMZ positively influences patient survival in GBM, especially in those with a methylated O^6-methylguanine DNA methyltransferase (MGMT)[31,32].

Radiological treatment assessment

Radiological assessment of treatment response in glioma was traditionally based on the bidimensional measurement of the area of enhancement[33], but the introduction of angiogenesis inhibitors (such as bevacizumab) has led to the diagnostic challenge of pseudoresponse: enhancement decreases or disappears because the tumour vasculature normalises and is therefore no longer permeable, while the tumour itself may not be responding to treatment. The RANO criteria[34] therefore now includes the assessment of non-enhancing in addition to enhancing lesions, which also make them applicable to non-enhancing, commonly lower grade, glioma. The time between scans is generally 6-12 weeks, but is sometimes increased in case of stable disease. A summary of the RANO criteria for both GBM and lower grade glioma can be found in ***Table 1***.

Table 1. Summary of the RANO criteria for glioblastoma (GBM) and low-grade glioma (LGG)[34,37].

Response	Criteria GBM	Criteria LGG
CR	*Requires all of the following*: complete disappearance of all enhancing (non-) measurable disease sustained for at least 4 weeks. No progression of non-enhancing disease. No new lesions. No corticosteroids. Stable or improved clinically.	*Requires all of the following*: complete disappearance of the lesion on T2w/ FLAIR images. No new lesions aside from radiation effects. No corticosteroids. Stable or improved clinically.
PR	*Requires all of the following*: ≥50% decrease in the sum of products of perpendicular diameters of all measurable enhancing lesions compared to baseline sustained for at least 4 weeks. No progression of non-enhancing disease. No new lesions. Stable or reduced corticosteroids. Stable or improved clinically.	*Requires all of the following*: ≥50% decrease in the sum of products of perpendicular diameters on Tw/FLAIR imaging compared to baseline sustained for at least 4 weeks. No new lesions aside from radiation effects. Stable or reduced corticosteroids. Stable or improved clinically.
Minor response	-	*Requires all of the following*: 25-50% decrease of non-enhancing lesion area on T2w/FLAIR images compared to baseline. No new lesions aside from radiation effects. Stable or reduced corticosteroids. Stable or improved clinically.
SD	Does not qualify for CR, PR or PD. Stable or reduced corticosteroids. Stable clinically.	Does not qualify for CR, PR, minor response or PD. No new lesions aside from radiation effects. Stable or reduced corticosteroids. Stable or improved clinically.
PD	*Requires any of the following*: ≥25% increase in the sum of products of perpendicular diameters of enhancing lesions compared to the smallest tumour measurement from earlier studies. Significant increase in non-enhancing lesions. Any new lesion. Clinical deterioration.	*Requires any of the following*: Development of new lesions or increase of enhancement. ≥25% increase of T2w/ FLAIR non-enhancing lesions while on stable or increasing steroid-dosage and not caused by radiotherapy or other. Clinical deterioration.

*CR=complete response, PR=partial response, SD=stable disease, PD=progressive disease.

Advanced methods of treatment assessment (MR imaging)

In a pretreatment setting, *diffusion MR imaging* derived parameters, such as ADC and FA, can aid in grading gliomas and localising areas of high cellularity suitable for biopsy[35]. After treatment, however, these parameters no longer correlate with cellular density, as they are influenced by other factors such as cell swelling and necrosis[36]. At a group level, ADC values still tend to be higher in gliomas than in normal appearing white matter (NAWM), but at an individual level there is considerable overlap and they are therefore not useful for response assessment[37].

Perfusion imaging derived rCBV and CBF in both grey and white matter are decreased after radiotherapy and can remain low for up to 6 and 9 months respectively in high-dose areas[38,39]. High rCBV values (>2.0 times that of the contralateral NAWM) can be used to distinguish tumour from pseudo-progression or radiation necrosis with reported sensitivities of up to 82% and specificity of 78%[40,41]. In diffuse astrocytoma, an increase in rCBV indicates malignant transformation[37]. In oligodendroglioma rCBV tends to be moderately increased even when low grade, but a further increase indicates malignant transformation[37].

MR spectroscopy shows (transient) changes in molecules and metabolites in relation to treatment-related changes, such as neuronal dysfunction, oedema, damage to oligodendrocytes, demyelination, and inflammatory effects. Metabolites such as NAA, Cr, Cho and Lac change during and after radiation. For instance, a decrease in NAA occurs early after radiotherapy co-occurring with an increase in Cho, which can remain present for up to 6 months[42-44]. Due to the transient nature of metabolite changes, MR spectroscopy results need to be either interpreted in combination with other measures (MR imaging and/or PET) or with repeated measures in time.

PET imaging

A higher *FDG* uptake by glioma is correlated with higher tumour grade and worse prognosis[45-47]. With the exception of pilocytic astrocytomas, WHO grade I and II grade gliomas are typically negative on FDG PET (uptake similar to or less than white matter), and consequently this tracer is not suitable for response evaluation of low-grade glioma[13]. On the other hand, increased levels of FDG uptake in enhancing brain lesions are correlated with tumour recurrence in anaplastic glioma and glioblastoma.

In recurrent high-grade glioma, the uptake of FDG has been shown to be predictive of tumour metabolic response to TMZ versus TMZ plus radiotherapy[48], and for predicting survival following anti-angiogenic therapy with bevacizumab[45].

Current *amino acid* PET data suggest that both a reduction of amino acid uptake and/or a decrease of the metabolically active tumour volume are signs of treatment response associated with improved long-term outcome[13]. Moreover, the amount of residual tracer uptake in FET PET after surgery/prior to chemoradiation of glioblastoma (within 7-20 days after surgery) has a strong prognostic influence, even after adjustment by multivariate survival analyses for the effects of treatment, MGMT promoter methylation and other patient and tumour-related factors (***Figure 1***)[49]. The experience with amino acid PET for monitoring after treatment in patients with WHO grade II glioma is however limited.

The prognostic value of early changes of FET uptake 6-8 weeks after postoperative radiochemotherapy in glioblastoma patients has been evaluated prospectively[50,51]. PET responders with a decrease in the TBR of more than 10% had a significantly

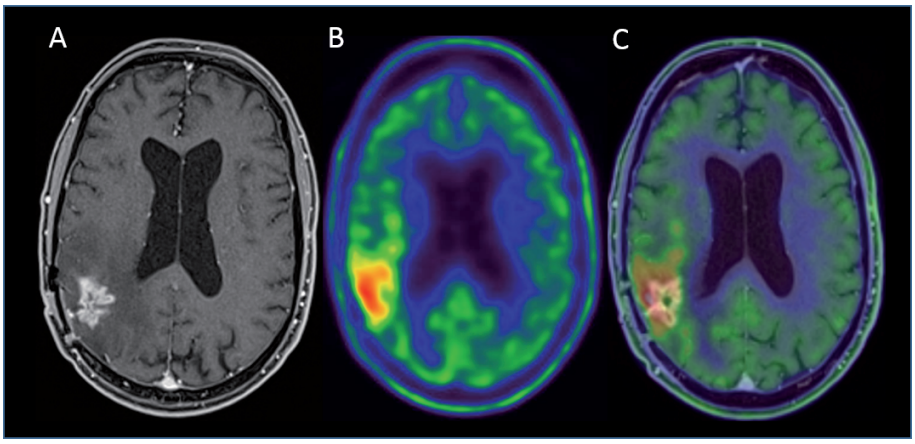

Figure 1. Neuroimaging studies of a patient with anaplastic astrocytoma performed 1 month after postoperative radiochemotherapy. An area of contrast enhancement on the T1w MR imaging sequence (**A**) is observed in the medial aspect of the residual surgical cavity. The MET-PET study (**B**) and MR imaging - PET fusion (**C**) show an absence of MET uptake in this part of the lesion ruling out the presence of tumour and indicating an area of pseudoprogression However, there is also an area of elevated MET uptake (TBR: 2.56) in the most lateral part of the lesion surrounding the area of pseudoprogression, suggesting the presence of infiltrative tumour relapse and as confirmed by biopsy.

longer disease-free and overall survival than patients with stable or increasing tracer uptake after radiochemotherapy. The kinetic analysis of FET uptake was not helpful in the evaluation of treatment effects to radiochemotherapy[50]. Patients with low-grade glioma evaluated 12 months after brachytherapy exhibit significantly reduced MET uptake[52,53]. For patients treated with alkylating chemotherapy, MET and FET PET may improve response assessment[54]. Reliable monitoring of temozolomide and nitrosourea-based chemotherapy (PCV scheme including procarbazine, CCNU and vincristine or CCNU monotherapy) has been demonstrated in patients with recurrent high-grade glioma[55]. Similarly, FET PET has been used to assess effects of TMZ according to the EORTC protocol 22033-26033 (application of 75 mg/m^2 TMZ per day over 21 days in a 28-day cycle)[56]. Additionally, a reduction of the metabolically active tumour volume after treatment initiation can be observed considerably earlier than volume reductions on FLAIR imaging[57]. Several studies suggest that treatment response and outcome in bevacizumab therapy can be assessed better with amino acid PET using 18F-FET and 18F-FDOPA than with MR imaging (see also ***section 4.2***)[58,59].

Lymphoma

Background

The classification of central nervous system (CNS) lymphoma now corresponds with the WHO 2016 classifications of systemic haematopoietic/lymphoid disease[60]. A

distinction is made between primary CNS lymphoma (PCNSL) and secondary CNS lymphoma. Secondary CNS lymphoma generally arises from aggressive non-Hodgkin lymphoma and has commonly (2/3) a leptomeningeal, and less commonly (1/3) a parenchymal localisation. PCNSL almost invariably has a parenchymal localisation. Typically, single or multiple contrast-enhancing lesions are seen surrounding the ventricles or in the corpus callosum[61]. Patients are treated with WBRT and multiple chemotherapeutic agents (including methotrexate) given both systemically and intrathecally or intraventricularly. Additionally steroids are given.

Radiological treatment assessment

Conventional treatment response assessment of brain parenchymal lymphoma is by contrast-enhanced MR imaging with an average time between follow-up scans of 2 months during therapy. The International Primary CNS Lymphoma Collaborative Group has determined response criteria in 2005. Complete response (CR) is determined by a lack of contrast-enhancement on MR imaging, no steroid-treatment and

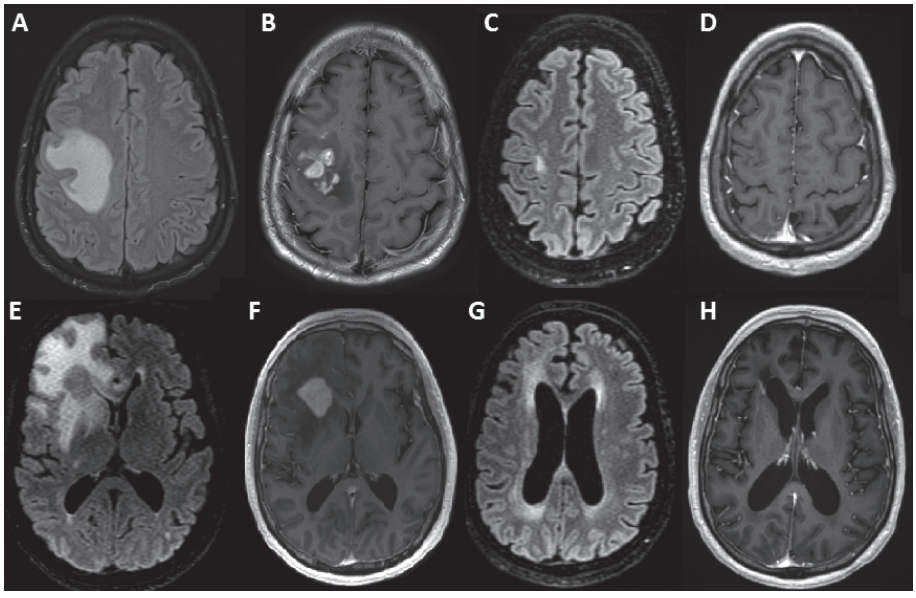

Figure 2. FLAIR and T1w post-contrast images in a 60-year old man with PCNSL in the right frontal lobe (**A** and **B**), treated with rituximab and MBVP followed by WBRT (30 Gy in 20 fractions) with resulting partial remission. Treatment continued with cytarabine and WBRT with SIB (30Gy in 20 fractions) and an additional boost on the tumour (10Gy in 20 fractions), resulting in complete remission with minimal white matter abnormalities considered to be a post-treatment effect (**C** and **D**). Recurrent disease four years later (**E** and **F**). After renewed treatment with MBVP and WBRT (20Gy in 5 fractions), a clear response was seen. Periventricular white-matter abnormalities and ex vacuo dilations of the ventricles is present as a post-treatment effect (**G** and **H**).

normal eye examination and cerebrospinal fluid (CSF) cytology. An unconfirmed complete response (CRu) is CR with minimal abnormalities on MR imaging and eye examination and/or any steroid use. Patients with a partial response (PR) have a 50% decrease of enhancing tumour without or only minor or decreasing eye disease with either negative or persistent/suspicious CSF cytology. Progressive disease (PD) is characterised by a ≥25% increase in enhancing lesions, new sites of disease, recurrent or new ocular disease and recurrent or positive CSF cytology[62]. Treatment response in parenchymal PCNSL is depicted in ***Figure 2***.

PET imaging

PCNSL often have high cellular density and consequently a markedly increased FDG uptake compared to other brain tumours, including glioblastoma and metastasis, and when compared to many infectious and inflammatory processes[13,63]. Cerebral infections such as toxoplasmosis and tuberculoma are a common differential diagnosis to PCNSL and exhibit a significantly lower uptake than patients with lymphoma, with no overlap of the uptake values (0.3-0.7 versus 1.7-3.1 respectively)[64,65].

There is no significant difference between MET PET and FDG PET in terms of sensitivity[66]. FDG PET has shown some clinical advantage in the differential diagnosis of lymphoma as most cerebral lymphomas have a high cell density and a high glucose metabolism, which is usually even higher than that of malignant gliomas and cerebral metastasis. In addition, FDG it is clinically more available and it can be performed as a whole-body scan for the assessment of systemic lymphoma involvement. Interestingly, FDG PET might also useful to demonstrate a response to chemotherapy in lymphoma patients very early after the initiation of therapy (***Figure 3***)[67].

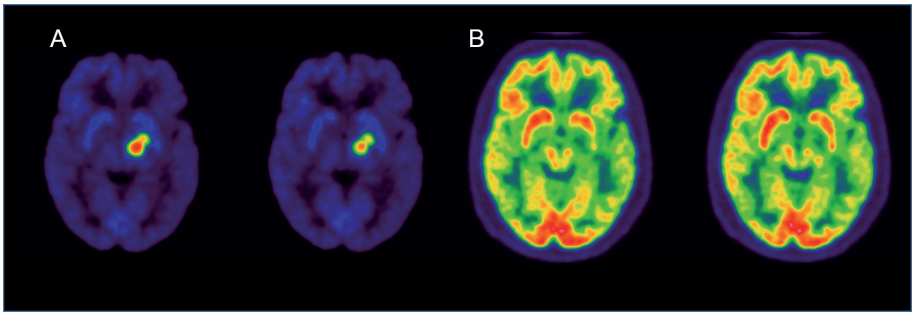

Figure 3. Brain FDG PET of primary CNS lymphoma at baseline (**A**), and 3 months after two cycles of chemotherapy (Carmustine, Methotrexate, Cytarabine, Rituximab according to the R-BAM scheme) and autologous hematopoietic stem cell transplantation (**B**) showing complete response.

Metastasis

Background

The main primary sites of brain metastases are lung, breast, and skin (melanoma). About 80% of brain metastases are located in the supratentorial brain (mainly frontal lobes) and about half of all patients have more than one metastases at the time of diagnosis[68]. Treatment consists of WBRT and/or stereotactic radiosurgery (SRS) depending on the size and number of lesions. Larger metastases may be surgically removed[69].

Radiological treatment assessment

The RANO Brain Metastases (RANO-BM) working group created radiological criteria for treatment assessment in clinical trials, which can also be used in clinical practice[70]. The metastases are categorised as target and non-target lesions. Target lesions are parenchymal metastases of at least 10x5 mm^2 in size. Up to five target lesions can be

Table 2. Response assessment in brain metastases: target and non-target lesions according to the RANO-group, radiological characteristics only[70].

Target lesions	**CR**	*Requires all of the following:* • Disappearance of all target lesions sustained for at least 4 weeks. • No new lesions. • No corticosteroids. • Stable or improved clinically.
	PR	*Requires all of the following* • ≥30% decrease in the sum of perpendicular diameters of target lesion size compared to the baseline sustained for at least 4 weeks. • No new lesions. • Stable or reduced corticosteroids. • Stable or improved clinically
	SD	Does not qualify for CR, PR of PD.
	PD	*Requires all of the following:* • ≥20% increase in the sum of longest diameters of target lesions compared to the smallest sum from earlier studies. • At least one lesion has increased ≥5mm.
Non-target lesions	**CR**	*Requires all of the following:* • Disappearance of all enhancing non-target lesions • No new lesions.
	PR/SD	Persistence of one or more non-target lesions.
	PD	*Requires any of the following*: • Unequivocal progression of existing enhancing non-target lesions. • New lesions (except while on immunotherapy-based treatment*) • Unequivocal progression of existing tumour-related non-enhancing (T2w/FLAIR) lesions.

*In case of immunotherapy-based treatment, new lesions alone may not constitute PD.

**CR=complete response, PR=partial response, SD=stable disease, PD=progressive disease.

measured. Non-target lesions include smaller parenchymal lesions, but also dural, leptomeningeal, and cystic (or non-measurable) lesions. In case of a mixed response to treatment, lesions that increase in size are considered leading. Recommended time between scans is 6-12 weeks. Aside from radiological features, the RANO-BM also includes clinical status and steroid dosage. The RANO-BM criteria can be found in ***Table 2***. Other response assessment methods include the RECIST criteria, in which lesions are measured in a single direction (≥30% decrease in the sum of diameters of the target lesions constitutes partial response, and a ≥20% increase progressive disease) and the WHO criteria, which include bi-dimensional measures (≥50% decrease in in the sum of the product of the diameters constitutes partial response, and ≥25% increase progressive disease). The appearance of a new lesion always indicates progressive disease[71].

PET imaging

PET imaging in the context of treatment assessment of metastasis is mostly used to distinguish tumour recurrence from treatment effects (see ***section3***).

FDG PET can add to the specificity for enhancing lesions that are equivocal or suspicious for recurrent tumour based on contrast-enhanced MR imaging alone in patients with brain metastases treated with SRS[72].

Meningioma

Background

The WHO classification distinguishes three grades of meningiomas: Grade I, or benign meningioma, constitute the vast majority (about 90%); Grade II (atypical) and grade III (malignant) meningiomas are considerably less common. Benign meningiomas can be eligible for (radio)surgery if the cause of symptoms. Radiotherapy can be considered in case of incomplete resection or at recurrence. Atypical and malignant meningiomas are surgically removed when possible and irradiated[60,73,74]. Both atypical and malignant meningiomas can metastasise to the lungs, liver and spine, although this is rare (0.1% of cases) and screening is therefore not routinely recommended[75].

Radiological treatment assessment

Meningiomas at risk for recurrence are those with pial invasion, and in the case of grade II and III meningioma when there is bone involvement or peritumoural oedema[76,77]. Meningiomas generally show intense homogeneous enhancement on post-contrast T1w images, and measurements are therefore performed on this sequence. Generally, the modified MacDonald criteria are used to determine treatment response, but it has been suggested that volumetric measures are more sensitive when it comes to

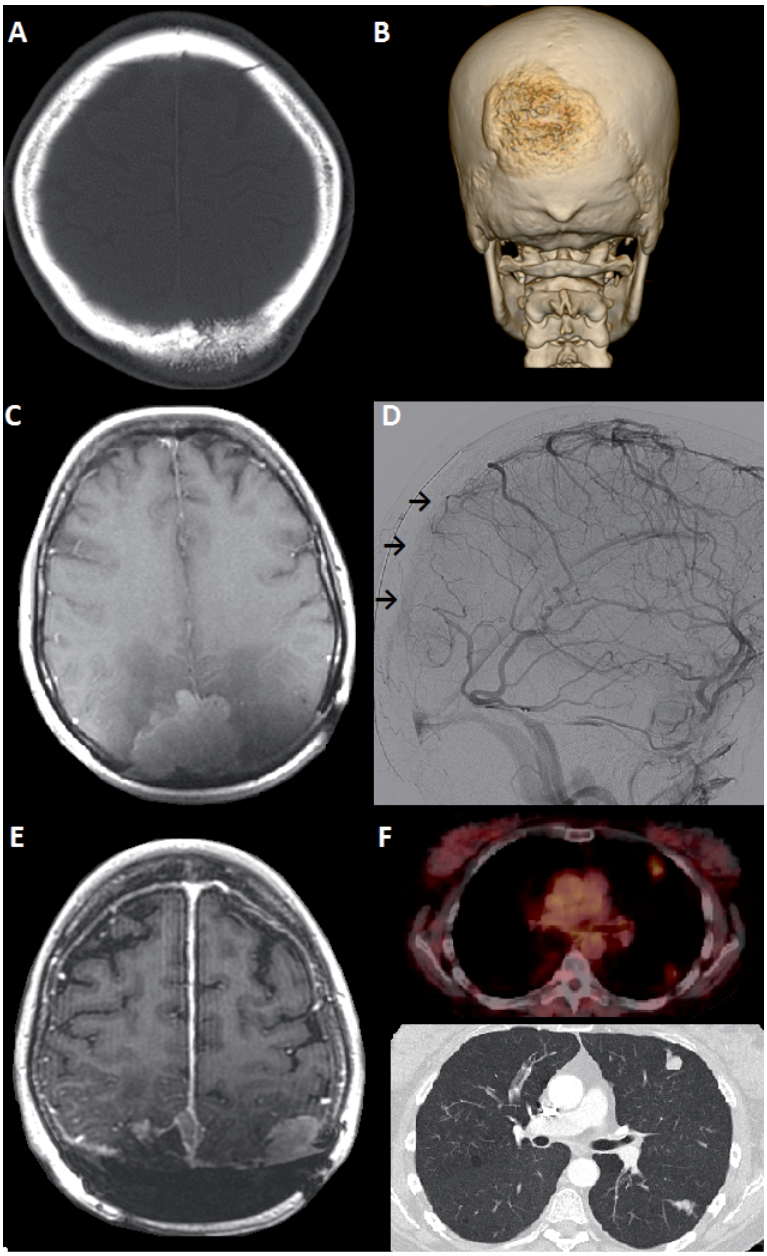

Figure 4. CT, MR imaging (T1w post-contrast), angiographic and FDG-PET images in a 40-year old woman with grade II meningioma primarily located in the skull (**A** and **B**). The tumour was resected and irradiated with 59.4Gy. Recurrent tumour growth appeared five years later intracranially (**C**) with compression of the superior sagittal sinus (**D**). Again, the tumour was resected. At second recurrence, multiple intracranial meningiomas appeared within the radiation field (**E**) and the patient was irradiated again (49.5Gy in 33 fractions). Aside from intracranial disease, the patient had histologically confirmed metastases in the lungs (**F**).

determining tumour growth due to the slow-growing nature of the tumours[78]. Additional meningiomas may appear in the course of time at other locations.

Early radiotherapy-related effects are tumour necrosis and oedema in the white matter[79]. Radiation-induced peritumoural changes occur in about 25% of patients, mainly in convexity, parasagittal and falx cerebri meningiomas after SRS[80]. Later radiotherapy-effects such as white matter abnormalities are often seen in high-dose areas and the periventricular white matter. An example of an irradiated patient with an atypical meningioma and its treatment course of depicted in ***Figure 4***.

PET imaging

The use of PET in meningioma patients is gradually increasing. Nevertheless, the usefulness of FDG PET is limited because meningiomas are mostly slow-growing and the metabolism of FDG is only elevated in atypical or anaplastic meningiomas[81].

MET PET scanning has been used to evaluate the effect of stereotactic high-energy proton beam treatment has been evaluated in a prospective study with 19 meningioma patients[82]. A reduction in the TBR was observed (even over several years) in the total patient group without a reduction in tumour size. Moreover, prior to the volume increase on MR imaging, MET uptake ratios were found to be increased, suggesting that treatment effects can be seen earlier than with CT or MR imaging[82].

Even though amino acid PET exhibits a better tumour-to-background contrast than FDG PET, the availability of specific SSTR ligands with even higher tumour-to-background contrast has led to a limited use of amino acid PET in meningioma assessment[54]. 68Ga-DOTA peptides PET have been shown more accurate than standard MR imaging to discriminate meningioma tissue from scar tissue related to pretreatment using both DOTATOC[83] and DOTATATE[20], even in transosseous extension of intracranial meningiomas[84]. Consequently, 68Ga-DOTA peptides may be useful in cases of unclear differential diagnosis between tumour progression and treatment-induced changes.

TREATMENT EFFECTS

Pseudo-progression and radiation necrosis

Background

Progressive disease can be mimicked by treatment-related toxicity from radiotherapy (pseudoprogression and radiation necrosis), immunotherapy, chemotherapy, and anti-epileptic drugs. Additional imaging techniques and sequential imaging combined with clinical characteristics may be needed to distinguish these entities from actual progressive disease[70,74]. Pseudoprogression occurs in a subacute setting after radiotherapy treatment combined with TMZ (within approximately 2-3

months after the start of treatment). Tumours with a methylated O^6-methylguanine DNA methyltransferase (MGMT) promotor respond best to TMZ. Initially it seemed that this group showed a higher incidence of pseudoprogression, but this has later been disputed[85]. Direct damage after radiotherapy is likely due to vasodilatation and increased capillary permeability, leading to disruption of the blood-brain-barrier and oedema. In case of pseudoprogression the response is excessive causing enhancement on post-contrast T1w images due to the damage to the blood-brain-barrier, and which is indistinguishable tumour progression[86.87].

Radiation necrosis is a chronic response to radiotherapy, which can occur from just months up to many years (median 1-2 years) after treatment; up to 90% occurs within the first 5 years posttreatment. There is endothelial damage**,** enzyme changes and immunological response leading tot necrosis. Radiation necrosis similar to pseudoprogression causes enhancement on post-contrast T1w images, mimicking tumour recurrence or progression[86,88].

The reported incidences of pseudoprogression and radiation necrosis vary widely, from 2% to 48%, depending on the source and the definition used. The incidence is influenced by radiation dose, field size, number of fractions, prior WBRT, chemotherapy (mainly cisplatin, carboplatin, doxorubicin, methotrexate, and temozolomide), immunotherapy, length of survival, age at time of radiotherapy, and diabetes mellitus[88].

Standard structural imaging

Distinguishing pseudoprogression and radiation necrosis from tumour residue or recurrence is challenging. Radiation-induced lesions can occur at the primary tumour site, but also at a distance, including the contralateral hemisphere, if included in the field of radiation. There is a predilection for white matter, especially the corpus callosum, because of the higher susceptibility of oligodendrocytes to radiation damage (compared to neurons) and relatively lower blood supply[89]. In patients with low-grade gliomas there is also a predilection for subependymal localisation[90]. The enhancing area is surrounded by oedema, which tends to be somewhat more extensive in radiation-induced lesions[91]. Different patterns of enhancement have been described, including nodular and rim enhancement with either regular or irregular margins and combined nodular and linear enhancing foci that create a mosaic-like appearance[88,92], but no reliable distinctive characteristics have been found. Radiation-induced lesions more often contain haemorrhagic lesions visible on T2*-weighted images, although these can also occur in glioma and metastases (especially malignant melanoma)[88]. To complicate things further, lesions containing both radiation damage and tumour commonly occur. Patients with multiple lesions can show a mixed response, which can indicate the presence of pseudoprogression or radiation necrosis. More advanced imaging techniques, follow-up and sometimes histopathological assessment are generally necessary to make the final diagnosis.

Advanced MR imaging

With *diffusion MR imaging*, ADC values tend to be lower in recurrent tumour compared to radiation necrosis at the group level, likely due to increased cellularity, but at the individual level these values overlap[93]. Comparing ADC measures from the enhancing and non-enhancing areas can be helpful: in case of tumour, the ADC values taken from the non-enhancing area tend to be significantly higher than those from the enhancing area, while in radiation necrosis ADC values from both enhancing and non-enhancing areas are similar[88]. DTI-derived FA values in enhancing areas tend to be higher in recurrent tumour than in radiation necrosis[94].

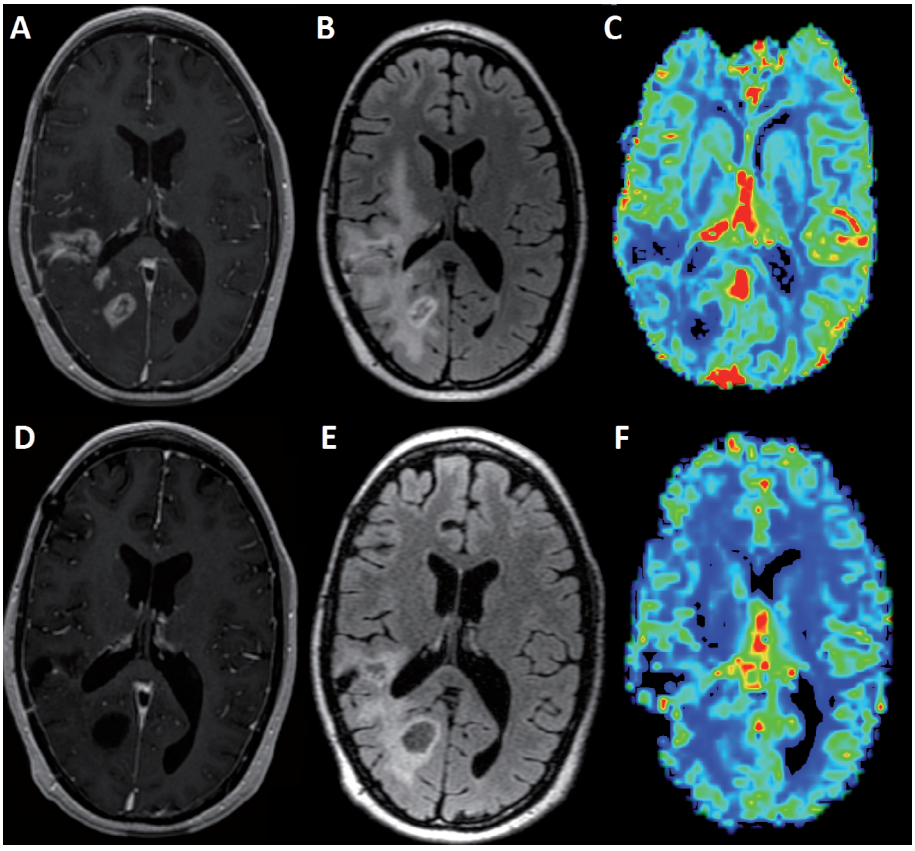

Figure 5. T1w post-contrast, FLAIR and DSC-perfusion rCBV maps in a glioblastoma patient with new enhancing lesions (**A**) and surrounding oedema (**B**) after prior treatment by the Stupp protocol. The rCBV map (**C**) shows low perfusion in the enhancing areas. The patient was enrolled in a clinical trial and treated with both bevacizumab and lomustine. At 6 weeks' follow-up the enhancement had disappeared (**D**) and the surrounding oedema was decreased (**E**). A small artefact is present on the rCBV map (**F**), but there is no evidence of increase in perfusion.

Perfusion-imaging derived rCBV is commonly assessed as a ratio of the area of interest over the normal appearing white matter (NAWM) in the contralateral hemisphere. In high-grade tumours and metastases the rCBV ratio is high, whereas in radiation necrosis/pseudoprogression the rCBV ratio is low. The proposed cut-off value lies between 1.5 and 2.6[40,41]. In about 8% of cases results are false-negative, as tumours can have rCBV ratios <1.5. Radiation necrosis can be safely diagnosed when the ratio is <0.6 (***Figure 5***)[41,95]. In current clinically used software it is easy to measure rCBV in multiple regions of interest (ROIs), but the interrater variability is quite large when it comes to deciding ROI size and placement. Other methods for measuring perfusion, such as using a different contrast-agent than gadolinium like ferumoxytol and using a different technique such as ASL are under investigation, showing promising results[96.97].

MR spectroscopy shows different metabolite concentrations in radiation necrosis from those measured in tumour. Reductions in individual metabolites Cho, Cr, and NAA indicate tissue damage and thus radiation necrosis. Favouring tumour are high ratios of Cho/Cr and Cho/NAA and low ratios of NAA/Cr and Lac/Cho. In order to distinguish tumour from radiation necrosis different cut-off values for these ratios have been proposed: Cho/Cr >1.5-1.8, Cho/NAA >1-1.8, and Lac/Cho <0.75-1.05[43,98,99]. Single voxel MR spectroscopy techniques requires precise placement of the voxel to be measured. In the presence of mixed tumour and radiation necrosis within the same voxel, tumour signal can be obscured because the metabolite concentration is averaged and then tends to suggest inflammatory changes[43]. Such partial volume effects can be reduced with multivoxel MRS, in which multiple small voxels are placed. It is sometimes also important to look at changes over time, because of certain transient changes in metabolite concentrations: Cho for instance can be temporality increased in radiation necrosis, falsely indicating tumour presence[99].

A relatively new method of measuring metabolites is *CEST*, which can potentially also be used to distinguish radiation damage from tumour: Amide proton transfer (APT), for instance, is found to be increased in tumour tissue[8]. CEST studies to date are still scarce and the true clinical value remains to be determined.

PET imaging

After radiation therapy, *FDG* can be used to distinguish radiation necrosis from recurrent glioma. Although different rates of diagnostic accuracy has been have been reported in the literature, FDG seems to be less sensitive than amino acid radiotracers with lower inter-observer agreement[100,101]. However, diagnostic accuracy increases when FDG is evaluated in combination with MR imaging (***Figure 6***)[102]. *Amino acid* PET radiotracers are useful for the differentiation between treatment related changes

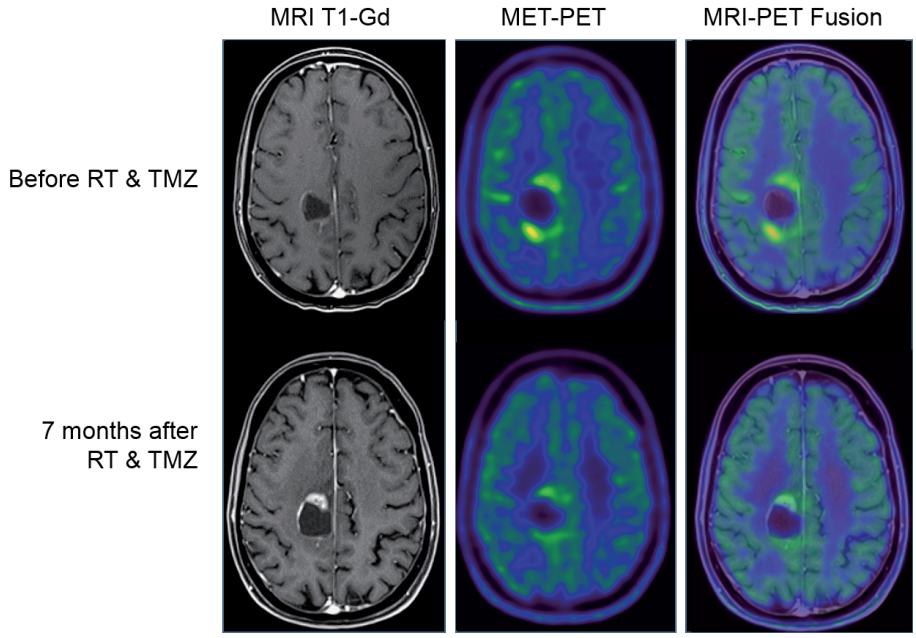

Figure 6. Patient with GBM studied before and after treatment (radiotherapy with concomitant temozolomide, and additional 6 cycles of temozolomide). An area of contrast enhancement on the T1w MR imaging sequence is observed in the anterior part of the cavity; there is only mild MET uptake (TBR=1.7; significantly lower than initial residual tumour with TBR= 2.6), consistent with radiation necrosis.

and true progression with higher diagnostic accuracy than standard MR imaging. [13] Recent studies with a larger glioblastoma patient cohort reported a diagnostic accuracy of FET PET of at least 85% for differentiating both typical (within 12 weeks) and late (> 12 weeks) pseudoprogression after radiochemotherapy completion from true tumour progression (***Figure 1***)[54].

Pseudoprogression after immunotherapy has been reported using FET PET in a small retrospective pilot study in patients with malignant melanoma brain metastasis treated with ipilimumab or nivolumab[103].

TBR, uptake kinetics and tumour volumes using FET PET have been evaluated for their value in monitoring stereotactic brachytherapy using iodine-125 seeds[104]. FET PET correctly differentiated with a high diagnostic accuracy late posttherapeutic effects after 6 months from local tumour progression in patients with recurrent high-grade glioma.

Comparison/combination of methods

Perfusion-derived and PET-derived measures are considered the most reliable when it comes to discerning tumour from radiation necrosis. ASL may be preferable over

DSC-perfusion imaging because it does not suffer from T1 leakage effects and it allows for quantitative measurement of CBF[97].

In clinical practice a combination of MR imaging sequences are used and they can be complementary. When the diagnosis is unclear based on MR imaging alone, PET-imaging can be considered. An ideal situation would be to use hybrid PET-MR imaging. Information on tissue perfusion, cellularity, integrity of neurons, anaerobic glycolysis during hypoxia, status of cellular membranes and metabolic pathways can then be acquired in one setting[5].

Angiogenesis inhibitors and pseudoresponse

Background

Angiogenesis inhibitors, such as the VEGF-inhibitor bevacizumab, are now used in variety of tumours including (recurrent) glioblastoma and meningioma. In addition, bevacizumab is now used to alleviate oedema surrounding the tumour, but also oedema due to radiation necrosis. Due to vascular normalisation 'leaky' tumour vasculature is normalised and new vessel growth is inhibited. This not only reduces oedema but also reduces or even complete dissolution of tumour enhancement. This phenomenon is known as pseudoresponse because the tumour may still present[107].

With radiation necrosis already difficult to distinguish from residual or recurrent tumour, the addition of angiogenesis inhibitors further complicates image interpretation as it can mask the tumour as well as reduce radiation necrosis effects. Varying or mixed response to the treatment between patients further plays a confounding role[108,109]. In the context of treatment for radiation necrosis, patients responding to bevacizumab treatment only infrequently show recurrence or progression of radiation necrosis after discontinuation[110].

PET imaging

The problem of accurately identifying non-enhancing tumour (pseudoresponse) has been investigated using amino acid PET to assess treatment response to antiangiogenic therapy[111]. Recent studies and case reports indicate that FET and FDOPA PET are useful in the context of pseudoresponse both detecting and ruling out the presence of tumour[54]. FET and FDOPA PET have also been used to predict a favourable outcome in responders to bevacizumab[54].

A cost effectiveness analysis of FET PET for therapy monitoring of antiangiogenic therapy suggests that the combined use of MR imaging and FET PET in the management of these patients have the potential to avoid overtreatment and corresponding costs, as well as unnecessary patient side effect[112].

LATE EFFECTS OF RADIOTHERAPY

In addition to radiation necrosis, radiotherapy has other late effects on the brain parenchyma, including demyelination, vascular abnormalities and atrophy. Radiation-induced tumours and malignant transformation have also been reported[87,113]. The extent of these effects is related to total radiation dose, field size, number of fractions and frequency, chemotherapy and other medication (methotrexate, corticosteroids, anti-epileptic drugs), patient survival and age at the time of radiation therapy[87].

White matter abnormalities

White matter is rich in glial cells, such as oligodendrocytes, which are more sensitive to radiation than neurons[43]. White matter damage is a common finding in irradiated patients and includes reactive gliosis, inflammation, oedema, demyelination, atrophy, coagulative necrosis, cavitation/cysts and calcification[87,114]. These different entities are difficult to distinguish on histological data and practically impossible to differentiate with MR imaging. White matter damage is visible as atrophy and/or T2w/FLAIR hyperintensity, also known as leukoencephalopathy[87,92]. The damage can be limited to small discrete lesions or there can be large confluent areas.

Radiation-induced damage to the white matter starts to appear on T2w/FLAIR images just months after treatment and is generally more severe in older patients[113]. Areas with limited blood supply, such as the periventricular white matter, are affected more than for instance the arcuate fasciculus which also receives cortical arterial supply[88,89]. Before abnormalities are visible on the T2w/FLAIR images, DTI can already pick up changes in white matter, using parameters such as MD, FA, and diffusivity perpendicular and parallel to the white matter fibres[115]. It has been postulated that some of these observed changes may be reversible[116].

Grey matter abnormalities

Because neurons are less sensitive to radiation than glial cells the grey matter is generally less affected than white matter. Effects that occur are cortical thinning, irregularity within the cortex (visible as T2w-hyperintensity) and blurring of the grey matter white matter junction[92,117]. Both grey and white matter damage can result in cognitive decline with deficits in learning, working memory and executive functions. Symptoms are more prominent when specific areas, such as the hippocampus and corpus callosum, are damaged[118].

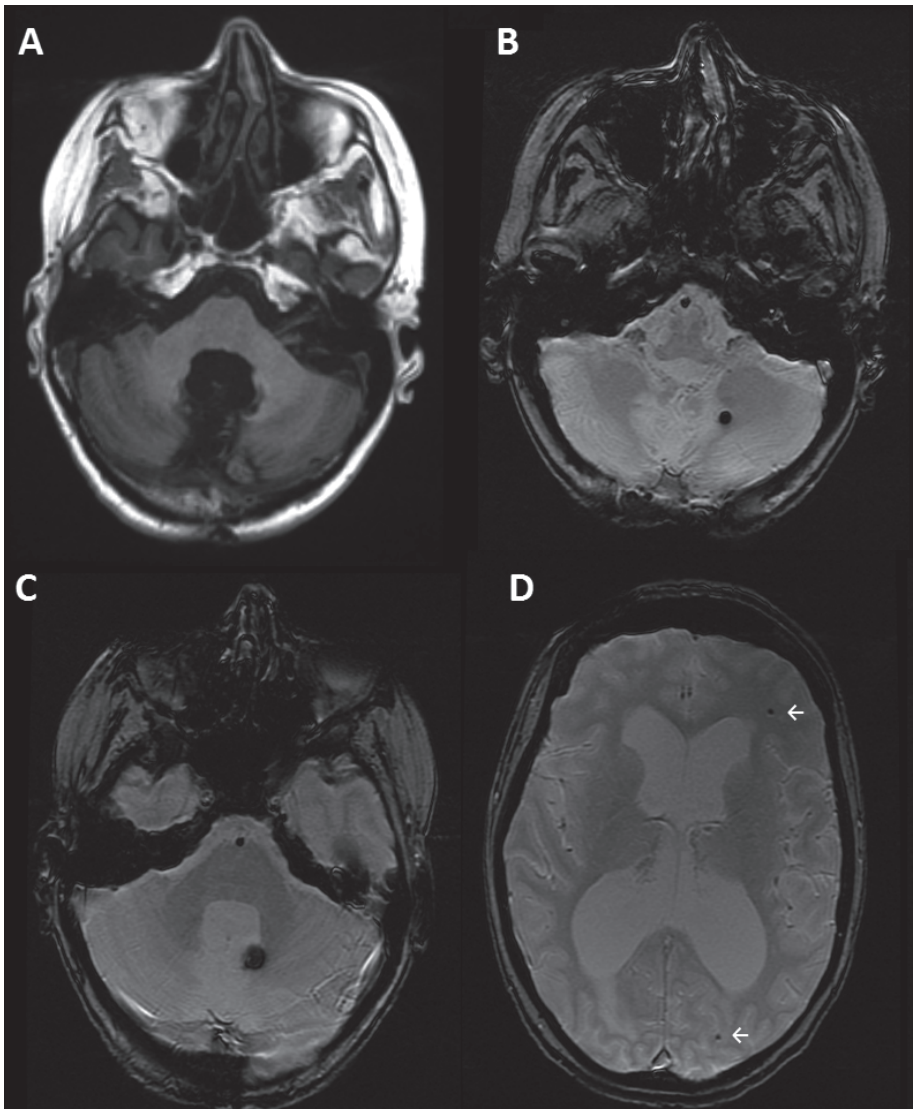

Figure 7. 35-year old woman treated for medulloblastoma 14 years ago. After subtotal resection, the tumour was irradiated (57.5Gy) and there has been no recurrent disease. T1w-image shows post-operative effects in the posterior fossa (**A**). The T2* (gradient echo) sequence shows multiple lesions with signal loss infra- and supratentorially (**B**, **C**, and **D**), consistent with cavernomas.

Vascular changes

Direct damage to endothelial cells leads to an increase in permeability, vasogenic oedema, ischemia and hypoxia. Complications that develop after four months include lacunar infarcts, microbleeds, large-vessel occlusions with moya-moya syndrome, (capillary) teleangiectasias, cavernomas (***Figure 7***), and stroke[86].

A rare late complication after radiotherapy is the so-called SMART syndrome: Stroke-like Migraine Attacks after Radiation Therapy (***Figure 8***). Patients have transient clinical symptoms and radiological findings suggestive of tumour recurrence such as unilateral enhancement of the cortex and T2w-hyperintense white matter. The posterior regions of the brain is predominantly involved. The effects are reversible[119].

Radiation-induced tumours and malignant transformation

A radiation-induced tumour is a new tumour that grows within the radiation field and different histology from the original tumour. Tumours most often encountered are meningiomas, followed by glioma and sarcoma[87,113]. The reported incidence of radiation-induced tumours is 2.6% in irradiated children. In adults however, the incidence is much lower[87,120].

Malignant transformation of meningioma due to irradiation is disputed. The reported incidence is 2.2%, but since malignant transformation of meningioma can also occur in the absence of radiotherapy, the true incidence is probably lower. Vestibular schwannoma has been reported to undergo malignant transformation due to radiation therapy in 0.3% of cases[73,121].

PET imaging

Treatment effects may decrease FDG uptake in the treatment area as well as in brain regions that receive synaptic input from the treated area.

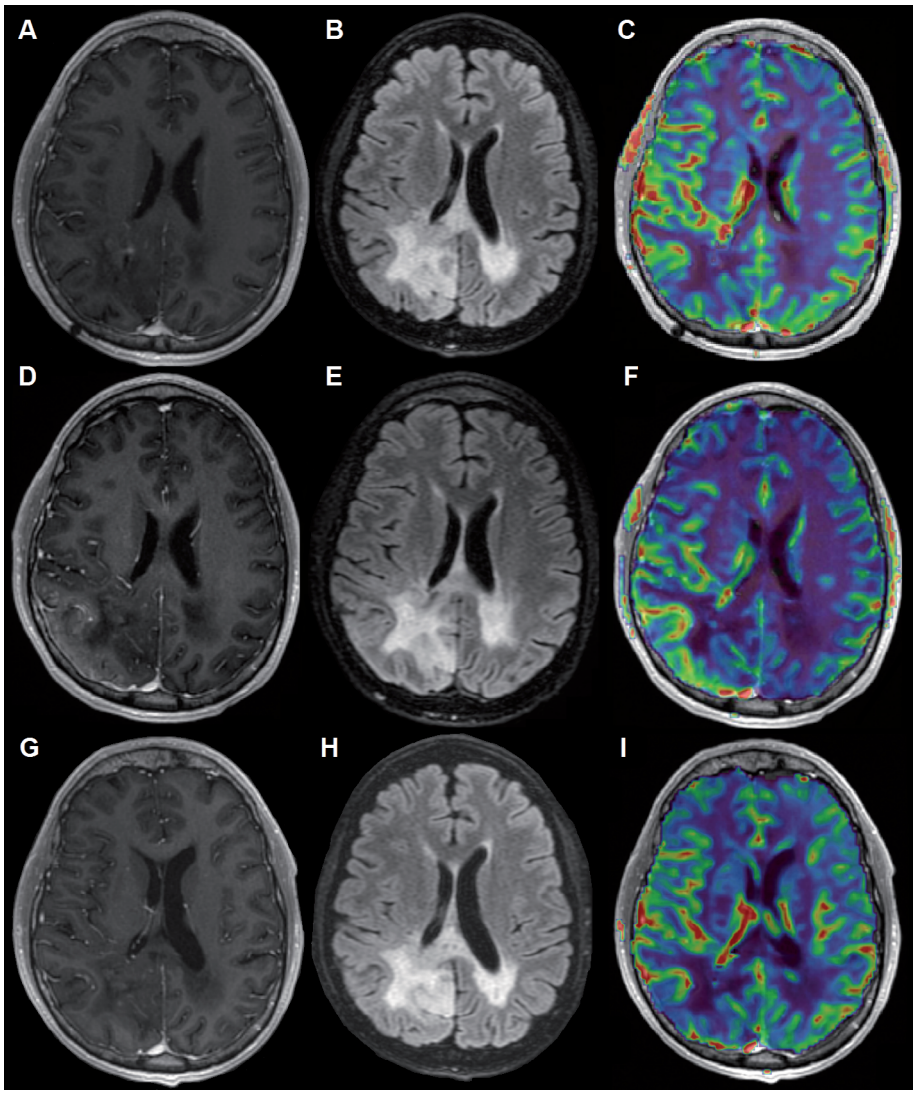

Figure 8. 43-year old male with oligodendroglioma initially treated with radiotherapy (50.4Gy) 6 years previously and with chemotherapy at progression 4 years later. T1w post-contrast (**A**), FLAIR (**B**), and rCBV (**C**) after therapy show stable residual abnormalities. The patient subsequently developed headaches and disorientation. On the T1w post-contrast image there is enhancement of the cortex (**D**) adjacent to the FLAIR hyperintense area (**E**). rCBV is increased in the enhancing area (**F**). At 2 months' follow-up imaging findings had regressed (**G**, **H**, **I**). Symptoms and imaging findings were consistent with SMART-syndrome.

REFERENCES

1. Symms M, Jager H, Schmierer M, Yousry T. A review of structural magnetic resonance neuroimaging. J Neurol Neurosurg Psychiatry 2004;75(9):1235-1244.
2. Soares JM, Marques P, Alves V, Sousa N. A hitchhiker's guide to diffusion tensor imaging. Fron Neurosci 2013;7:31.
3. Shim WH, Kim HS, Choi C-G, Kim SJ. Comparison of apparent diffusion coefficient and intravoxel incoherent motion for differentiating among glioblastoma, metastasis, and lymphoma focusing on diffusion-related parameter. PLoS One 2015;10(7):e134761.
4. Paulson ES, Schmainda KM. Comparison of dynamic susceptibility-weighted contrast-enhanced MR methods: recommendations for measuring relative cerebral blood volume in brain tumors. Radiology 2008;249(2):601-613.
5. Ferda J, Ferdova E, Hes O, Mracek J, Kreuzberg B, Baxa J. PET/MRI: multiparametric imaging of brain tumors. Eur J Radiol 2017;94:A14-A25.
6. Cebeci H, Aydin O, Ozturk-Isik E, et al. Assessment of perfusion in glial tumors with arterial spin labelling; comparison with dynamic susceptibility contrast method. Eur J Radiol 2014;83(10):1914-1919.
7. Horska A, Barker PB. Imaging of brain tumors: MR spectroscopy and metabolic imaging. Neuroimaging Clin N Am 2010;20(3):293-310.
8. Kogan F, Hariharan H, Reddy R. Chemical exchange saturation transfer (CEST) imaging: description of technique and potential clinical applications. Curr Radiol Rep 2013;1(2):102-114.
9. Sugo N, Yokota K, Kondo K, et al. Early dynamic 201TI SPECT in the evaluation of brain tumours. Nuclear Medicine Communications 2006;27(2):143-149.
10. Prigent-Le Jeune F, Dubois F, Perez S, Blond S, Steinling M. Technetium-99m sestamibi brain SPECT in the follow-up of glioma for evaluation of response to chemotherapy: first results. Eur J Nucl Med Mol Imaging 2004;31(5):714-719.
11. Varrone A, Asenbaum S, van der Borght T, et al. EANM procedure guidelines for PET brain imaging using [18F]FDG, version 2. Eur J Nucl Med Mol Imaging 2009;36(12):2103-2110.
12. Herholz K, Langen KJ, Schiepers C, Mountz JM. Brain tumors. Semin Nucl Med 2012;42(6):356-370.
13. Albert NL, Weller M, Suchorska B, et al. Response Assessment in Neuro-Oncology working group and European Association for Neuro-Oncology recommendations for the clinical use of PET imaging in gliomas. Neuro Oncol 2016;18(9):1199-1208.
14. Bergström M, Collins VP, Ehrin E, et al. Discrepancies in brain tumor extent as shown by computed tomography and positron emission tomography using [68Ga]EDTA, [11C]glucose, and [11C]methionine. J Comput Assist Tomogr 1983;7(6):1062-1066.
15. Aki T, Nakayama N, Yonezawa S, et al. Evaluation of brain tumors using dynamic 11C-methionine-PET. J Neurooncol 2012;109(1):115-122.
16. Calcagni NL, Galli G, Giordano A, et al. Dynamic O-(2-[18F]fluorethyl)-L-tyrosine (F-18 FET) PET for glioma grading: assessment of individual probability of malignancy. Clin Nucl Med 2011;36(10):841-847.
17. Ceccon G, Lohmann P, Stoffels G, et al. Dynamic O-(2-18F-fluorethyl)-L-tyrosine positron emission tomography differentiates brain metastasis recurrence from radiation injury after radiotherapy. Neuro Oncol 2017;19(2):281-288.
18. Langen KJ, Watts C. Neuro-oncology: amino acid PET for brain tumours – ready for the clinic? Nat Rev Neurol 2016;12(7):375-376.

19. Dutour A, Kumar U, Panetta R, et al. Expression of somatostatin receptor subtypes in human brain tumors. Int J Cancer 1998;76(5):620-627.

20. Rachinger W, Stoecklein VM, Terpolilli NA, et al. Increased 68Ga-DOTATATE uptake in PET imaging discriminates meningioma and tumor-free tissue. J Nucl Med 2015;56(3):347-353.

21. Galldiks N, Albert NL, Sommerauer M, et al. PET imaging in patients with meningioma-report of the RANO/PET group. Neuro oncol 2017;19(12):1576-1587.

22. Chen W, Delaloye S, Silverman DH, et al. Predicting treatment response of malignant gliomas to bevacizumab and irinotecan by imaging proliferation with [18F] fluorothymidine positron emission tomography: a pilot study. J Clin oncol 2007;25(30):4714-4721.

23. Wardak M, Schiepers C, Cloughesy TF, Dahlbom M, Phelps ME, Huang SC. ^{18}F-FLT and ^{18}F-FDOPA PET kinetics in recurrent brain tumors. Eur J Nucl Med Mol Imaging 2014;41(6):1199-1209.

24. Lee ST, Scott AM. Hypoxia positron emission tomography imaging with 18f-fluoromisonidazole. Semin Nucl Med 2007;37(6):451-461.

25. Spence AM, Muzi M, Swanson KR, et al. Regional hypoxia in glioblastoma multiforme quantified with [18F]fluoromisonidazole positron emission tomography before radiotherapy: correlation with time to progression and survival. Clin Cancer Res 2008;14(9):2623-2630.

26. Su Z, Roncaroli F, Durrenberger PF, et al. The 18-kDa mitochondrial translocator protein in human gliomas: an 11C-(R):PK11195 PET imaging and neuropathology study. J Nucl Med 2015;56(4):512-517.

27. Awde AR, Bolsgard R, Theze B, et al. The translocator protein radioligand 18F-DPA-714 monitors antitumor effect of erufosine in a rat 9L intracranial glioma model. J Nucl Med 2013;54(12):2125-2131.

28. Gomez-Rio M, Testart Dardel N, Santiago Chinchilla A, et al. ^{18}F-Fluorocholine PET/CT as a complementary tool in the follow-up of low-grade glioma: diagnostic accuracy and clinical utility. Eur J Nucl Med Mol Imaging 2015;42(6):886-895.

29. Rottenburger C, Hentschel M, Kelly T, et al. Comparison of C-11 methionine and C-11 choline for PET imaging of brain metastases: a prospective pilot study. Clin Nucl Med 2011;36(8):639-642.

30. Stupp R, Brada M, van den Bent MJ, et al. High-grade glioma: ESMO Clinical Practice Guidelines for diagnosis, treatment and follow-up. Ann Oncol 2014;25 Suppl 3:iii93-101.

31. Nifterik van KA, van den Berg J, Stalpers LJ, et al. Differential radiosensitizing potential of temozolomide in MGMT promotor methylated glioblastoma multiforme cell lines. Int J Radiat Oncol Biol Phys 2007;69(4):1246-1253.

32. Chalmers AJ, Ruff EM, Martindale C, Lovegrove N, Short SC. Cytotoxic effects of temozolomide and radiation are additive- and schedule-dependent. Int J Radiat Oncol Phys 2009;75(5):1511-1519.

33. Macdonald DR, Cascino TL, Schold SC Jr, Cairncross JG. Response criteria for phase II studies of supratentorial malignant glioma. J Clin Oncol 1990;8(7):1277-1280.

34. Wen PY, Macdonald DR, Reardon DA, et al. Updated response assessment criteria for high-grade gliomas: response assessment in neuro-oncology working group. J Clin Oncol 2010;28(11):1963-1972.

35. Inoue T, Ogasawara K, Beppu T, Ogawa A, Kabasawa H. Diffusion tensor imaging for preoperative evaluation of tumor grade in gliomas. Clin Neurol Neurosurg 2005;107(3):174-180.

36. Tsien C, Cao Y, Chenevert T. Clinical applications for diffusion magnetic resonance imaging in radiotherapy. Semin Radiat Oncol 2014;24(3):218-226.

37. Bent van den MJ, Wefel JS, Schiff D, et al. Response assessment in neuro-oncology (a report of the RANO group): assessment of outcome in trials of diffuse low-grade gliomas. Lancet Oncol 2011;12(6):583-593.

38. Fuss M, Wenz F, Scholdei R, et al. Radiation-induced regional cerebral blood volume (rCBV) changes in normal brain and low-grade astrocytomas: quantification and time and dose-dependent occurrence. Int J Radiat Oncol Biol Phys 2000;48(1):53-58.

39. Petr J, Platzek I, Seiditz A, et al. Early and late effects of radiochemotherapy on cerebral blood flow in glioblastoma patients measured with non-invasive perfusion MRI. Radiother oncol 2016;118(1): 24-28.

40. Kong DS, Kim ST, Kim EH, et al. Diagnostic dilemma of pseudoprogression in the treatment of newly diagnosed glioblastomas: the role of assessing relative cerebral blood flow volume and oxygen-6-methylguanine-DNA-methyltransferase promotor methylation status. AJNR Am J Neuroradiol 2011;32(2):382-387.

41. Sugahara T, Korogi Y, Tomiguschi S, et al. Posttherapeutic intraaxial brain tumor: the value of perfusion-sensitive contrast-enhanced MR imaging for differentiating tumor recurrence from nonneoplastic contrast-enhancing tissue. AJNR Am J Neuroradiol 2000;21(5):901-909.

42. Peca C, Pacelli R, Elefante A, et al. Early clinical and neuroradiological worsening after radiotherapy and concomitant temozolomide in patients with glioblastoma: tumour progression or radionecrosis? Clin Neuro Neurosurg 2009;111(4):331-334.

43. Sundgren PC. MR spectroscopy in radiation injury. AJNR Am J Neuroradiol 2009;30(8):1469-1476.

44. Walecki J, Sokol M, Pieniazek P, et al. Role of short TE 1H-MR spectroscopy in monitoring of postoperation irradiated patients. Eur J Radiol 1999;30(2):154-161.

45. Colavolpe C, Chinot O, Metellus P, et al. FDG-PET predicts survival in recurrent high-grade gliomas treated with bevacizumab and irinotecan. Neuro Oncol 2012;14(5):649-657.

46. Dunet V, Pomoni A, Hottinger A, Nicod-Lalonde M, Prior JO. Performance of 18F-FET versus 18F-FDG-PET for the diagnosis and grading of brain tumors: systematic review and meta-analysis. Neuro Oncol 2016;18(3):426-434.

47. Mertens K, Acou M, van Hauwe J, et al. Validation of 18F-FDG PET at conventional and delayed intervals for the discrimination of high-grade from low-grade gliomas: a stereotactic PET and MRI study. Clin Nucl Med 2013;38(7):495-500.

48. Charnley N, West CM, Barnett CM, et al. Early change in glucose metabolic rate measured using FDG-PET in patients with high-grade glioma predicts response to temozolomide but not temozolomide plus radiotherapy. Int J Radiat Oncol Biol Phys 2006;66(2):331-338.

49. Suchorska B, Jansen NL, Linn J, et al. Biological tumor volume in 18FET-PET before radiochemotherapy correlated with survival in GBM. Neurology 2015;84(7):710-719.

50. Piroth MD, Pinkawa M, Holy R, et al. Prognostic value of early [18F]fluoroethyltyrosine positron emission tomography after radiochemotherapy in glioblastoma multiforme. Int J Radiat Oncol Biol Phys 2011;80(1):176-184.

51. Galdiks N, Langen KJ, Holy R, et al. Assessment of treatment response in patients with glioblastoma using O-(2-18F-fluoroethyl)-L-tyrosine PET in comparison to MRI. J Nucl Med 2012;53(7): 1048-1057.

52. Voges J, Herholz K, Hölzer T, et al. 11C-methionine and 18F-2-fluorodeoxyglucose positron emission tomography: a tool for diagnosis of cerebral glioma and monitoring after brachytherapy with 125I seeds. Stereotact Funct Neurosurg 1997;69(1-4 Pt2):129-135.

53. Würker M, Herholz K, Voges J, et al. Glucose consumption and methionine uptake in low-grade gliomas after iodine-125 brachytherapy. Eur J Nucl Med 1996;23(5):583-586.

54. Galdiks N, Law I, Pope WB, Arbizu J, Langen KJ. The use of amino acid PET and conventional MRI for monitoring of brain tumor therapy. Neuroimage Clin 2016;13:386-394.

55. Galdiks N, Kracht LW, Burghaus L, et al. Use of 11C-methionine PET to monitor the effects of temozolomide chemotherapy in malignant gliomas. Eur J Nucl Med Mol Imaging 2006;33(5):516-524.

56. Wyss M, Hofer S, Bruehlmeier M, et al. Early metabolic responses in temozolomide treated low-grade glioma patients. J Neuroncol 2009;95(1):87-93.

57. Roelcke U, Wyss M, Nowosielski M, et al. Amino acid positron emission tomography in monitor chemotherapy response and predict seizure control and progression-free survival in WHO grade II gliomas. Neuro Oncol 2016;18(5):744-751.

58. Galdiks N, Rapp M, Stoffels G, et al. Response assessment of bevacizumab in patients with recurrent malignant glioma using [18F]Fluoroehtyl-L-tyrosine PET in comparison to MRI. Eur J Nucl Med Mol Imaging 2013;40(1):22-33.

59. Schwarzenberg J, Czernin J, Cloughesy TF, et al. Treatment response evaluation using 18F-FDOPA PET in patients with recurrent malignant glioma on bevacizumab therapy. Clin Cancer Res 2014; 20(13):3550-3559.

60. Louis DN, Perry A, Reifenberger G, et al. The 2016 World Health Organization Classification of Tumor of the Central Nervous System: a summary. Acta Neuropathol 2016;131(6):803-820.

61. Haldorsen IS, Espeland A, Larsson EM. Central nervous system lymphoma: characteristic findings on traditional and advanced imaging. AJNR Am J Neuroradiol 2011;32(6):984-892.

62. Abrey LE, Batchelor TT, Ferreri AJ, et al. Report of an international workshop to standardize baseline evaluation and response criteria for primary CNS lymphoma. J Clin Oncol 2005;23(22): 5034-5043.

63. Makino K, Hirai T, Nakamura H, et al. Does adding FDG-PET to MRI improve the differentiation between primary cerebral lymphoma and glioblastoma? Observer performance study. Ann Nucl Med 2011;25(6):432-438.

64. Hoffman JM, Waskin HA, Schifter T, et al. FDG-PET in differentiating lymphoma from nonmalignant central nervous system lesions in patients with AIDS. J Nucl Med 1993;34(4):567-575.

65. Sathekge M, Goethals I, Maes A, van de Wiele C. Positron emission tomography in patients suffering from HIV-1 infection. Eur J Nucl Med Mol Imaging 2009;36(7):1176-1184.

66. Kawase Y, Yamamoto Y, Kameyama R, Kawai N, Kudomi N, Nishiyama Y. Comparison of 11C-methionine PET and 18F-FDG PET in patients with primary central nervous system lymphoma. Mol Imaging Biol 2011;13(6):1284-1289.

67. Kawai N, Miyake K, Yamamoto Y, Nishiyama Y, Tamiya T. 18F-FDG PET in the diagnosis and treatment of primary central nervous system lymphoma. Biomed Res Int 2013;2013:247152.

68. Nussbaum ES, Djalillian HR, Cho KH, Hall WA. Brain metastases. Histology, multiplicity, surgery, and survival. Cancer 1996;78(8):1781-1788.

69. Lippitz B, Lindquist C, Paddick I, Peterson D, O'Neill K, Beaney R. Stereotactic radiosurgery in the treatment of brain metastases: the current evidence. Cancer Treat Rev 2014;40(1):48-59.

70. Lin NU, Lee EQ, Aoyama H, et al. Response assessment criteria for brain metastases: proposal from the RANO group. Lancet Oncol 2015;16(6):e270-278.

71. Lin NU, Lee EQ, Aoyama H, et al. Challenges relating to solid tumour brain metastases in clinical trials, part 1: patient population, response, and progression. A report from the RANO group. Lancet Oncol 2013;14(10):e396-406.

72. Belohlavek O, Simonova G, Kantorova I, Novotny J Jr, Liscak R. Brain metastases after stereotactic radiosurgery using the Leksell gamma knife: can FDG PET help to differentiate radionecrosis from tumour progression? Eur J Nucl Med Mol Imaging 2003;30(1):96-100.

73. Rogers L, Barani I, Chamberlain M, et al. Meningiomas: knowledge base, treatment outcomes, and uncertainties. A RANO review. J Neurosurg 2015;122(1):4-23.

74. Alexiou GA, Gogou P, Markoula S, Kyritsis AP. Management of meninigomas. Clin Neurol Neurosurg 2010;112(3):177-182.

75. Kessler RA, Garzon-Muvdi T, Yang W, et al. Metastatic atypical and anaplastic meningioma: a case series and review of the literature. World Neurosurg 2017;101:47-56.

76. Nowak A, Dziedzic T, Krych P, Czernicki T, Kunert P, Marchel A. Benign versus atypical meningiomas: risk factors predicting recurrence. Neurol Neurochir Pol 2015;49(1):1-10.

77. Gabeau-Lacet D, Aghi M, Betensky RA, Barker FG, Loeffler JS, Louis DN. Bone involvement predicts poor outcome in atypical meningioma. J Neurosurg 2009;111(3):464-471.

78. Quant EC, Wen PY. Response assessment in neuro-oncology. Curr Oncol Rep 2011;13(1):5056.

79. Lee SR, Yang KA, Kim SK, Kim SH. Radiation-induced intratumoral necrosis and peritumoral edema after gamma knife radiosurgery for intracranial meningiomas. J Korean Neurosurg Soc 2012;52(2): 98-102.

80. Chang JH, Chang JW, Chol JY, Park YG, Chung SS. Complications after gamma knife radiosurgery for benign meningiomas. J Neurol Neurosurg Psychiatry 2003;74(2):226-230.

81. Cremerius U, Bares R, Weis J, et al. Fasting improves discrimination of grade 1 and atypical or malignant meningioma in FDG-PET. J Nucl Med 1997;38(1):26-30.

82. Ryttlefors M, Danfors T, Latini F, Montelius A, Blomquist E, Gudjonsson O. Long-term evaluation of the effect of hypofractionated high-energy proton treatment of benign meningiomas by means of (11)C-L-methionine positron emission tomography. Eur J Nucl Med Mol Imaging 2016;43(8): 1432-1443.

83. Afshar-Oromieh A, Giesel FL, Linhart HG, et al. Detection of cranial meningiomas: comparison of ^{88}Ga-DOTATOC PET/CT and contrast-enhanced MRI. Eur J Nucl Med Mol Imaging 2012;39(9): 1409-1415.

84. Kunz WG, Jungblut LM, Kazmierczak PM, et al. Improved detection of transosseous meningioma using 66Ga-DOTATATE PET/CT compared with constrast-enhanced MRI. J Nucl Med 2017;58(10): 1580-1587.

85. Wick W, Chinot OL, Bendszus M, et al. Evaluation of pseudoprogression rates and tumor progression patterns in a phase III trial of bevacizumab plus radiotherapy/temozolomide for newly diagnosed glioblastoma. Neuro Oncol 2016;18(10):1434-1441.

86. Brandsma D, Stalpers L, Taal W, Sminia P, van den Bent MJ. Clinical features, mechanisms, and management of pseudoprogression in malignant gliomas. Lancet Oncol 2008;9(5):453-461.

87. Martino A, Krainik A, Pasteris C, et al. Neurological imaging of brain damages after radiotherapy and/or chimiotherapy. J Neuroradiol 2014;41(1):52-70.

88. Raimbault A, Cazals X, Lauvin MA, Destrieux C, Chapet S, Cottier JP. Radionecrosis of malignant glioma and cerebral metastasis: a diagnostic challenge in MRI. Diagn Interv Imaging 2014;95(10): 985-1000.

89. Kumar AJ, Leed NE, Fuller GN, et al. Malignant gliomas: MR imaging spectrum of radiation therapy- and chemotherapy-induced necrosis of the brain after treatment. Radiology 2000;217(2):377-384.

90. West van SE, de Bruin HG, van de Langerijt B, Swaak-Kragten AT, van den Bent MJ, Taal W. Incidence of pseudoprogression in low-grade gliomas treated with radiotherapy. Neuro Oncol 2017; 19(5):719-725.

91. Leeman JE, Clump DA, Flickinger JC, Mintz AH, Burton SA, Heron DE. Extent of perilesional edema differentiated radionecrosis from tumor recurrence following stereotactic radiosurgery for brain metastases. Neuro Oncol 2013;15(12):1732-1738.

92. Chan YL, Leung SF, King AD, Choi PH, Metreweli C. Late radiation injury to the temporal lobes: morphologic evaluation at MR imaging. Radiology 1999;213(3):800-807.

93. Castillo M, Smith JK, Kwock L, Wilber K. Apparent diffusion coefficients in the evaluation of high-grade cerebral gliomas. AJNR Am J Neuroradiol 2001;22(1):60-64.

94. Xu JL, Li YL, Lian JM, et al. Distinction between postoperative recurrent glioma and radiation injury using MR diffusion tensor imaging. Neuroradiology 2010;52(12):1193-1199.

95. Hu LS, Baxter LC, Smith KA, et al. Relative cerebral blood volume values to differentiate high-grade glioma recurrence from posttreatment radiation effect: direct correlation between image-guided tissue histopathology and localized dynamic susceptibility-weighted contrast-enhanced perfusion MR imaging measurements. AJNR Am J Neuroradiol 2009;30(3):552-558.

96. Gahramanov S, Raslan AM, Muldoon LL, et al. Potential for differentiation of pseudoprogression from true tumor progression with dynamic susceptibility-weighted contrast-enhanced magnetic resonance imaging using ferumoxytol vs. gadoteridol: a pilot study. Int J Radiat Oncol Biol Phys 2011;79(2):514-523.

97. Ozsunar Y, Mullins ME, Kwong K, et al. Glioma recurrence versus radiation necrosis? A pilot comparison of arterial spin-labeled dynamic susceptibility contrast enhanced MRI, and FDG-PET imaging. Acad Radiol 2010;17(3):282-290.

98. Elias AE, Carlos RC, Smith EA, et al. MR spectroscopy using normalized and non-normalized metabolite ratios for differentiating recurrent brain tumor from radiation injury. Acad Radiol 2011; 18(9):1101-1108.

99. Nakajima T, Kumabe T, Kanamori M, et al. Differential diagnosis between radiation necrosis and glioma progression using sequential proton magnetic resonance spectroscopy and methionine positron emission tomography. Neurol Med Chr (Tokyo) 2009;49(9):394-401.

100. Dankbaar JW, Snijders TJ, Robe PA, et al. The use of ^{18}F-FDG PET to differentiate progressive disease from treatment induced necrosis in high grade glioma. J Neurooncol 2015;125(1):167-175.

101. Laere van K, Ceyssens S, van Calenbergh F, et al. Direct comparison of 18F-FDG and 11C-methionine PET in suspected recurrence of glioma: sensitivity, inter-observer variability and prognostic value. Eur J Nucl Med Mol Imaging 2005;32(1):39-51.

102. Santra A, Kumar R, Sharma P, et al. F-18 FDG PET-CT in patients with recurrent glioma: comparison with contrast enhanced MRI. Eur J Radiol 2012;81(3):508-513.

103. Kebir S, Rauschenbach L, Galldiks N, et al. Dynamic O-(2-[18F]fluoroethyl)-L-tyrosine PET imaging for the detection of checkpoint inhibitor-related pseudoprogression in melanoma brain metastases. Neuro Oncol 2016;18(10):1462-1464.

104. Jansen NL, Suchorska B, Schwarz SB, et al. [18F]fluoroethyltyrosine-positron emission tomography-based therapy monitoring after stereotactic iodine-125 brachytherapy in patients with recurrent high-grade glioma. Mol Imaging 2013;12(3):137-147.

105. Brandsma D, van den Bent MJ. Pseudoprogression and pseudoresponse in the treatment of gliomas. Curr Opin Neurol 2009;22(6):633-638.

106. Norden AD, Young GS, Setayesh K, et al. Bevacizumab for recurrent malignant gliomas: efficacy, toxicity, and patterns of recurrence. Neurology 2008;70(10):779-787.

107. Nayak L, Iwamoto FM, Rudnick JD, et al. Atypical and anaplastic meninigomas treated with bevacizumab. J Neurooncol 2012;109(1):187-193.

108. Gonzalez J, Kumar AJ, Conrad CA, Levin VA. Effect of bevacizumab on radiation necrosis of the brain. Int J Radiat Oncol Biol Phys 2007;67(2):232-236.

109. Sanborn MR, Danish SF, Rosenfeld MR, O'Rourke D, Lee JY. Treatment of steroid refractory, Gamma Knife related radiation necrosis with bevacizumab: case report and review of the literature. Clin Neurol Neurosurg 2011;113(9):798-802.

110. Levin VA, Bidaut L, Hou P, et al. Randomized double-blind placebo-controlled trial of bevacizumab therapy for radiation necrosis of the central nervous system. Int J Radiat Oncol Biol Phys 2011; 79(5):1487-1495.

111. Reithmeier T, Lopez WO, Spehl TS, et al. Bevacizumab as salvage therapy for progressive brain stem gliomas. Clin Neurol Neurosurg 2013;115(2):165-169.

112. Heinzel A, Müller D, Langen KJ, et al. The use of O-(2-18F-fluoroethyl)-L-tyrosine PET for treatment management of bevacizumab and irinotecan in patients with recurrent high-grade glioma: a cost-effectiveness analysis. J Nucl Med 2013;54(8):1217-1222.

113. Johannesen TB, Lien HH, Hole KH, Lote K. Radiological and clinical assessment of long-term brain tumour survivors after radiotherapy. Radiother Oncol 2003;69(2):169-176.

114. Schultheiss TE, Kun LE, Ang KK, Stephens LC. Radiation response of the central nervous system. Int J Radiat Oncol Biol Phys 1995;31(5):1093-1112.

115. Nagesh V, Tsien CI, Chenevert TL, et al. Radiation-induced changes in normal-appearing white matter in patients with cerebral tumors: a diffusion tensor imaging study. Int J Radiat Oncol Biol Phys 2008;70(4):1002-1010.

116. Tsui EY, Chan JH, Ramsey RG, et al. Late temporal lobe necrosis in patients with nasopharyngeal carcinoma: evaluation with combined multi-section diffusion weighted and perfusion weighted MR imaging. Eur J Radiol 2001;39(3):133-138.

117. Seibert TM, Karunamuni R, Kaifi S, et al. Cerebral cortex regions selectively vulnerable to radiation dose-dependent atrophy. Int J Radiat Oncol Biol Phys 2017;97(5):910-918.

118. Saad S, Wang TJ. Neurocognitive deficits after radiation therapy for brain malignancies. Am J Clin Oncol 2015;38(6):634-640.

119. Zheng Q, Yang L, Tan L-M, Qin L-X, Wang C-Y, Zhang H-N. Stroke-like migraine attacks after radiation therapy syndrome. Chin Med J (Engl) 2015;128)15):2097-2101.

120. Pollocl BE, Link MJ, Stafford SL, Parney IF, Garces YI, Foote RL. The risk of radiation-induced tumors or malignant transformation after single-fraction intracranial radiosurgery: results based on a 25-year experience. Int J Radiat Oncol Biol Phys 2017;97(5):919-923.

121. Al-Mefty O, Kadri PA, Pravdenkova S, Sawyer JR, Strangeby C, Husain M. Malignant progression in meningioma: documentation of a series and analysis of cytogenetic findings. J Neurosurg 2004; 101(2):210-218.